

Rainfall estimation for the south shore of the Mediterranean Sea using MSG infrared images

Mohsene A. TEBBI*¹, Boualem HADDAD¹

Accepted 15th August 2014

DOI: 10.18201/ijisae.16558

Abstract: The objective of this paper is the estimation of rainfall over the Algerian territory using MSG (Meteosat Second Generation) infrared data. To achieve this aim, we applied a calibrated GPI (GOES Precipitation Index) approach. This technique is tested to the complex situation of the Mediterranean climate. The rainfall estimated is obtained by using an affectation of adapted rain rates for a brightness temperature. These rain rates are determinate by analysing two years of in situ measures. The tests have been concluded during the rainy months January, February, and September of 2006/2007. The results show a good correlation between measured and estimated rainfall in winter and summer where stratiform and convective cells are present.

Keywords: Meteorological satellite, Mediterranean climate, IR MSG images data, Convective and Stratiform clouds, GPI approach.

Introduction

Meteorological satellites are the only instruments used to monitor rainfall field whatever is the nature of the ground (oceans, seas, desert, mountains,...etc). The estimation of rainfall from satellite imagery began in the first launches.

Several programs have been developed and applied to estimate the rainfall such as GPCP (Global Precipitation Climate Project) [1] and TRMM (Tropical Rainfall Measuring Mission) [2]. In French, EPSAT program (Estimation of Precipitation using Satellite) has the objective to study satellite rainfall estimates on countries in West Africa where rain is a crucial parameter. Techniques researching the relationship between thermal infrared and rainfall intensity have been widely used [3]-[4]-[5]-[6]. Some works combine IR data with microwaves data to enhance the estimation, but these are not usually provided by all geostationary satellites [7]-[8]. The most techniques are mainly applied to tropical regions where rainfall is largely provided by convective cells. IR satellite techniques were used in the western Mediterranean region in various conditions and with variety of aims [9]. The south shore of the Mediterranean sea presents a complex climate. Indeed, the stratiform and convective precipitations coexist. Some authors have suggested to use optical and microphysical parameters to estimate the precipitations in this case[10]-[11]. In the recent past, Tarruella and Joge have shown that we can adapt the Arkin (GPI) and NAW (Negri Adler Wesley) techniques for estimating rainfall in the Mediterranean region[9]. The question is: can we adapt the GPI method to the south shore of the Mediterranean Sea?

Our contribution in this paper is to propose an algorithm capable to estimate precipitations in Algeria using only infrared data of 10.8 μ m channel. It is GPI approach calibrated, adapted for this

complex situation.

1. Study region and datasets

1.1 Study region

The study region is the Algerian territory boarded on the east by Tunisia and Libya, on the South by Niger and Mali, South-West by Mauritania and West by Morocco.

This region is characterized by two types of climate. In the north, the climate is Mediterranean and the average rainfall is estimated about 600 mm. The climate is Arid in the South and the average rainfall is minimum and about 50 mm. The rainy season is extended from October to March. In summer, the convective systems are observed.

1.2 MSG/SEVIRI Infrared data

The satellite data used are provided by the national office of meteorology of Algeria (ONM) located in Algiers, which equipped with a receiving station of SEVIRI data. The images used are obtained in infrared waves of 10.8 μ m by SEVIRI radiometer. Its spatial resolution is about 3 \times 3 km and the temporal resolution is one image every 15 minutes. Over northern Algeria, the satellite viewing zenith angle of SEVIRI is about 26 $^\circ$, and as a consequence the spatial resolution is reduced to about 4 \times 5 km². The raw image has a size of 3712 \times 3712 pixel. Series of 96 images constitute information of one day started at 6:00 a.m. and finished at 5:45 a.m. of next day.

The value of a pixel referred to as "count", is converted into radiance using a linear relation calibrated with corresponding calibration data provided with images. For each pixel, brightness temperature T_b (Kelvin) in infrared channel is calculated also with that data by using the formula of Planck [12].

1.3 In situ rain-gauge data

The rain-gauges data consist of measures of 55 rain-gauges distributed over the study region as illustrated by Fig. 1. The measures give the cumulated intensities in the daily scale.

¹ Laboratory of image processing and radiation, University of sciences and technology Houari Boumediene, 32, El Alia, Bab Ezzouar, 16111, Algiers, Algeria

* Corresponding Author: Email: tebbi@hotmail.fr

Note: This paper has been presented at the International Conference on Advanced Technology&Sciences (ICAT'14) held in Antalya (Turkey), August 12-15, 2014.

To localise the rain positions on satellite images, we convert GPS coordinates to pixel coordinate.

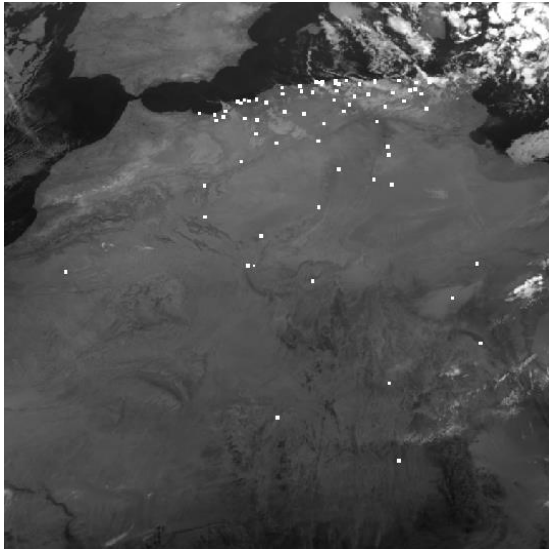


Figure 1. Geographical positions of Algerian rain-gauge network after the transformation of GPS coordinate to pixel coordinate

2. Technique description and results

The technique is based on infrared data. The determination of the cumulated rainfall is obtained using a correct affectation for a brightness temperature.

To determinate the best rain rate, we analysed a period of two years of the rainfall intensities in the various points of the study area. It was noted that it rains more in the East than in the West. We than assigned a value of 2 and 3.1 for the east region, and 1.2 and 2.7 for the western region respectively for winter and summer.

The brightness temperature for a given rain-gauge station correspond at a weighted mean of a 5×5 grid of pixels. The central pixel superposed on rain-gauge location has the most weight “5”. The neighbour pixels around the central pixel have less important weight and we affect the weight of “2”. Finally, the neighbour pixels of neighbour pixels have a less important weight “1/4”. The final brightness temperature information of each rain-gauge is given by (1).

$$WMBT^G = \frac{1}{25} \sum_{i=1}^5 \sum_{j=1}^5 W(i,j) \times T(i,j) \quad (1)$$

Where,

- $WMBT^G$: is the weighted mean brightness temperature.
- $W(i,j)$: is the weights matrix.
- $T(i,j)$: is the brightness temperature of pixel (i,j).

Weights matrix is given by (2)

$$W(i,j) = \begin{bmatrix} 1/4 & 1/4 & 1/4 & 1/4 & 1/4 \\ 1/4 & 2 & 2 & 2 & 1/4 \\ 1/4 & 2 & 5 & 2 & 1/4 \\ 1/4 & 2 & 2 & 2 & 1/4 \\ 1/4 & 1/4 & 1/4 & 1/4 & 1/4 \end{bmatrix} \quad (2)$$

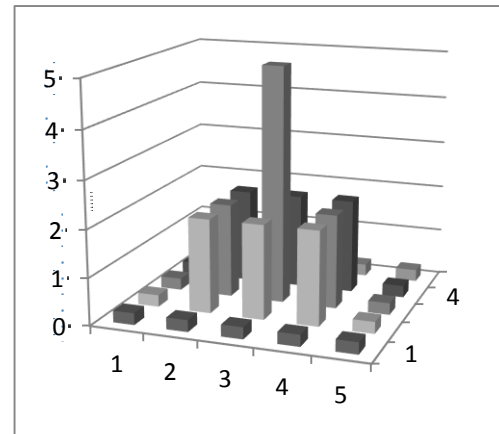


Figure 2. A 3-D representation of weights matrix

Several temperature thresholds are tested. We find that the values 263 ° K and 240 ° K are respectively the most suitable for winter and summer in this study. Also, we compared our results with original GPI approach [5]-[8].

The original GPI method uses a linear relationship between the fraction of an area with clouds colder than 235K and the rain accumulated over the target area in the tropical Atlantic Ocean.

The cumulated rainfall is calculated by (3).

$$GPI (mm) = RR \times Fc \times T \quad (3)$$

Where,

- GPI : is the cumulated rainfall in a given period.
- RR : is the proportionally constant equal to 3 mm/h.
- Fc : is the fractional coverage of pixel that its brightness temperature is ≤ 235 K (in our case we recalibrate this value with 263 K).
- T : is the number of hours of the analyzed period.

The application on rainy days of January, February, March and September 2007 gave some results as follows in Fig.3, 4, 5 and 6. Two different data sets have been correlated to analyze the potential of the above technique. The accumulated rain measured at each of 55 observatories of the main rain gauge was compared with the rain estimated by GPI calibrated over three months of winter and one month of summer. The superposition of the estimated rainfall and real rain gauge data show a good correlation.

Fig. 3, 4, 5 and 6 show the evolution of rainfall estimated by GPI calibrated and measured in situ. We note that they follow the same trend. We obtain a higher correlation coefficient for January, February and March and an acceptable correlation coefficient in summer.

To test the efficient of the approach, we calculated the bias, the root mean square error (RMSE) and the mean absolute error (MAE) which are defined as follows:

$$Bias = \frac{1}{N} \sum_{i=1}^N (Xi' - Xi) \quad (4)$$

$$RMSE = \sqrt{\frac{1}{N} \sum_{i=1}^N (Xi' - Xi)^2} \quad (5)$$

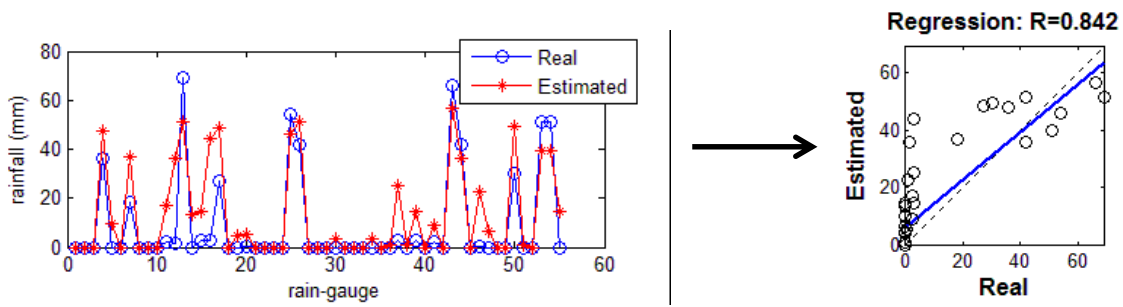


Figure 3. Superposition of estimated values of cumulated rainfall and rain gauge data for January 2007

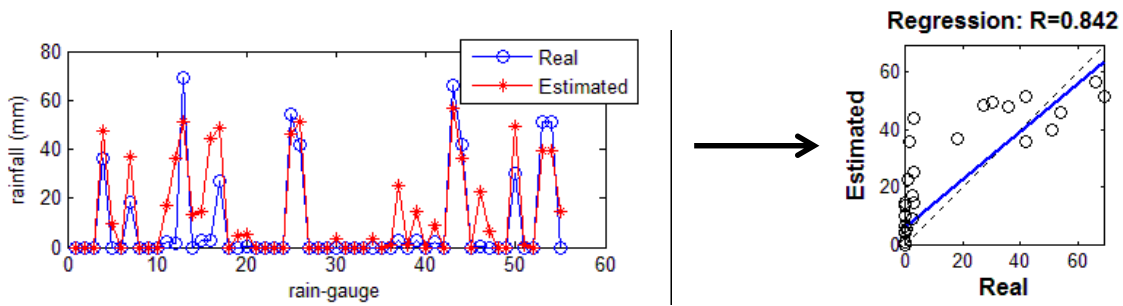


Figure 4. Superposition of estimated values of cumulated rainfall and rain gauge data for February 2007

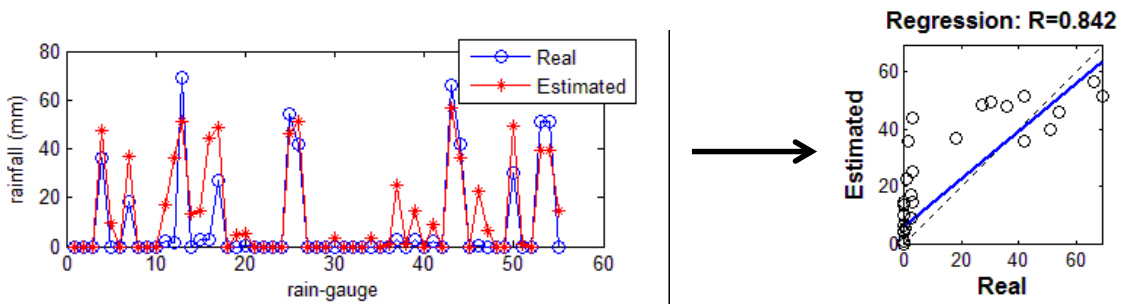


Figure 5. Superposition of estimated values of cumulated rainfall and rain gauge data for March 2007

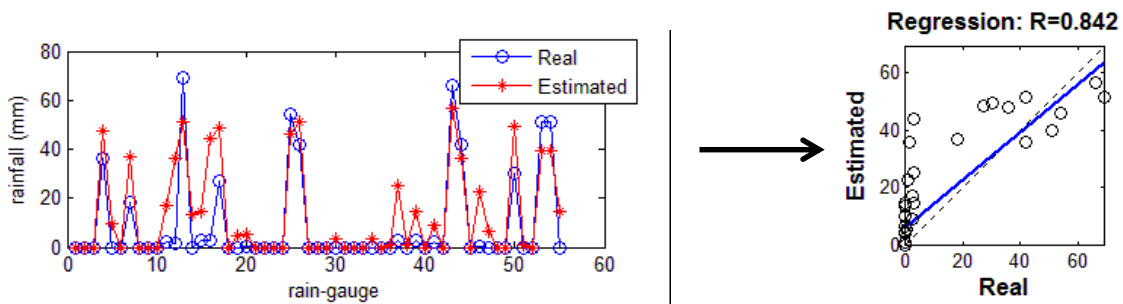


Figure 6. Superposition of estimated values of cumulated rainfall and rain gauge data for September 2007

$$MAE = \frac{1}{N} \sum_{i=1}^N |X'i - Xi| \quad (5)$$

Where,

- $X'i$: is the estimated value of rainfall for rain-gauge i .
- Xi : is the real value of rainfall for rain-gauge i .
- N : is total rain-gauges (55).

Table 1. Comparison between original GPI and calibrated GPI (W)

Time Errors	January 2007		February 2007		March 2007		September 2007	
	GP I	W	GP I	W	GP I	W	GP I	W
Bias (mm/m onth)	16.9	9.6	11.5	-3.9	22.2	-7	18	13.5
RMSE (mm/m onth)	32.6	23	31	18	33.9	15.4	29.1	24.7
MAE (mm/m onth)	23.4	13.8	16.7	9.5	18	6.5	19.4	14.6

Table 1 shows that our approach presents the smallest bias, defined as the difference between the measured and the estimated rainfall. Therefore, the bias is positive (negative) if the technique overestimates (underestimates) the precipitations. We then deduce that the GPI calibrated overestimates and underestimates slightly rainfall for the four months. In addition, MAE and RMSE values are much lower than those obtained by the approach GPI. The proposed approach seems better adapted for the south shore of the Mediterranean Sea.

Conclusion

The GPI approach is essentially adapted for convective cells. The stratiform clouds cover in winter the northern region of Algeria, while the convective systems are especially present in summer and autumn.

Analysis of the results shows that the proposed approach significantly improves the rainfall estimation whatever the season. In addition, the highest correlation coefficient and the lowest bias are obtained for the months of January, February and March during which the stratiform rains are frequent. We can therefore conclude that the proposed approach is well suited to the Mediterranean climate. Estimation errors are mainly due to Cirrus clouds whose brightness temperature is below the used thresholds.

The main advantage of this technique is that it is based on infrared data which are available frequently on the most of the earth regions from geostationary satellites and in orbit polar. We have shown that the IR data also provide interesting results. It is recommended to test this approach over a long period and to extend this study with an algorithm who allows more differentiation between rainy and no-rainy pixels on infrared images in order to minimise the error in estimation.

References

- [1] R. F. Adler, G. J. Huffman, A. Chang, R. Ferraro, P.-P. Xie, J. Janowiak, B. Rudolf, U. Schneider, S. Curtis, D. Bolvin, A. Gruber, J. Susskind, P. Arkin, et E. Nelkin, "The Version-2 Global Precipitation Climatology Project (GPCP) Monthly Precipitation Analysis (1979–Present)," *J. Hydrometeorol.*, vol. 4, n° 6, p. 1147–1167, déc. 2003.
- [2] J. S. Ojo et T. V. Omotosho, "Comparison of 1-min rain rate derived from TRMM satellite data and raingauge data for microwave applications in Nigeria," *J. Atmospheric Sol.-Terr. Phys.*, vol. 102, p. 17–25, sept. 2013.
- [3] A. K. Mishra, R. M. Gairola, A. K. Varma, et V. K. Agarwal, "Improved rainfall estimation over the Indian region using satellite infrared technique," *Adv. Space Res.*, vol. 48, n° 1, p. 49–55, juill. 2011.
- [4] R. F. Adler et A. J. Negri, "A satellite infrared technique to estimate tropical convective and stratiform rainfall," *J. Appl. Meteorol.*, vol. 27, n° 1, p. 30–51, 1988.
- [5] P. A. Arkin, "The Relationship between Fractional Coverage of High Cloud and Rainfall Accumulations during GATE over the B-Scale Array," *Mon. Weather Rev.*, vol. 107, n° 10, p. 1382–1387, oct. 1979.
- [6] A. T. Haile, T. Rientjes, A. Gieske, et M. Gebremichael, "Multispectral remote sensing for rainfall detection and estimation at the source of the Blue Nile River," *Int. J. Appl. Earth Obs. Geoinformation*, vol. 12, Supplement 1, p. S76–S82, févr. 2010.
- [7] R. F. Adler, A. J. Negri, P. R. Keehn, et I. M. Hakkarinen, "Estimation of monthly rainfall over Japan and surrounding waters from a combination of low-orbit microwave and geosynchronous IR data," *J. Appl. Meteorol.*, vol. 32, n° 2, p. 335–356, 1993.
- [8] L. Xu, X. Gao, S. Sorooshian, P. A. Arkin, et B. Imam, "A Microwave Infrared Threshold Technique to Improve the GOES Precipitation Index," *J. Appl. Meteorol.*, vol. 38, n° 5, p. 569–579, mai 1999.
- [9] R. Tarruella et J. Jorge, "Comparison of three infrared satellite techniques to estimate accumulated rainfall over the Iberian Peninsula," *Int. J. Climatol.*, vol. 23, n° 14, p. 1757–1769, 2003.
- [10] M. Lazri, S. Ameur, J. M. Brucker, J. Testud, B. Hamadache, S. Hameg, F. Ouallouche, et Y. Mohia, "Identification of raining clouds using a method based on optical and microphysical cloud properties from Meteosat second generation daytime and nighttime data," *Appl. Water Sci.*, vol. 3, n° 1, p. 1–11, mars 2013.
- [11] T. Nauss et A. A. Kokhanovsky, "Discriminating raining from non-raining clouds at mid-latitudes using multispectral satellite data," *Atmos Chem Phys*, vol. 6, n° 12, p. 5031–5036, nov. 2006.
- [12] (2013) EUMETSAT- MSG Level 1.5 Image Data Format Description. [Online]. Available: <https://www.eumetsat.int/website/home/Data/Products/Formats/index.html>